Examination of Inconsistencies in the Physical Modeling of Vapor-Liquid Interfaces of Strongly Non-Ideal Mixtures

Florian Fleckenstein,[†] Max Wagner,[†,‡] Thomas Bernet,[‡] Erich A. Müller,[‡] and Simon Stephan[*,†]

†Molecular Thermodynamics Group (MTG), RPTU Kaiserslautern, Erwin-Schrödinger-Straße 44, 67663 Kaiserslautern, Germany

‡Department of Chemical Engineering, Sargent Center for Process Systems Engineering, Imperial College London, South Kensington Campus, London SW7 2AZ, United Kingdom

E-mail: simon.stephan@rptu.de

Supplementary Information

Examination of Inconsistencies in the Physical Modeling of Vapor-Liquid Interfaces of Strongly Non-Ideal Mixtures

Florian Fleckenstein[a], Max Wagner[a,b], Thomas Bernet[b], Erich A. Müller[b], Simon Stephan[a,]*

[a]Molecular Thermodynamics Group (MTG), RPTU Kaiserslautern,

Erwin-Schrödinger-Straße 44, 67663 Kaiserslautern, Germany

[b]Department of Chemical Engineering, Sargent Center for Process Systems Engineering,

Imperial College London, South Kensington Campus, London SW7 2AZ, United Kingdom

*simon.stephan@rptu.de

October 20, 2025

The Supplementary Information for the publication *Examination of Inconsistencies in the Physical Modeling of Vapor-Liquid Interfaces of Strongly Non-Ideal Mixtures* contains

- an overview of the available experimental VLE data and experimental surface tension data for the studied systems, cf. Table S1,
- a more detailed view of the MD density profiles for the mixture cyclohexane + ethanol,
- a discussion on adjusted cross-interaction influence parameters,
- a comparison of the predictions from the stabilized and reference fluid DGT algorithm,
- a comparison of experimental VLE data to EOS calculations for the remaining mixtures not shown in the main body of this work,
- the p-T projections of the remaining mixtures not shown in the main body of this work,
- an example of the evaluation of the clustering of alcohol molecules within the molecular dynamics simulations,
- a detailed view on the component density profiles obtained from DFT for the mixture cyclohexane + ethanol,
- a comparison of the interfacial properties calculated from both equations of state in combination with DGT and DFT as well as MD results for the mixture cyclohexane + 2-propanol,
- the component density profiles of the mixture cyclohexane + 2-propanol from different equations of state in combination with DGT,
- the component density profiles of the mixtures not presented in the main body of this work for the PCP-SAFT EOS in combination with DGT and DFT,

- a detailed description of the component density profiles as the type 'iv' behavior changes to a monotonic transition for the sCPA and Peng-Robinson EOS,
- the numerical values of the MD simulation results for the mixtures cyclohexane + ethanol and cyclohexane + 2-propanol,
- and the numerical values of all component density profiles shown in the main body and Supplementary Information of this work.

1 Literature Overview over Experimental Surface Tension and VLE Data

Table S1 gives an overview of the literature experimental data on the VLE of the binary systems (cyclohexane / methylcyclohexane + ethanol / 2-propanol / 1-propanol / 1-butanol) in the temperature range 293.15 to 313.15 K.

Table S1: Literature overview of experimental VLE data of the binary systems (cyclohexane + 2-propanol / ethanol / 1-propanol / 1-butanol) and (methylcyclohexane + 2-propanol / ethanol / 1-propanol / 1-butanol) in the temperature range 293.15 to 313.15 K.

author	T / K	p / MPa
cyclohexane + ethanol		
VLE data		
Matteoli & Lepori[1]	298.15	
Cancellu et al.[2]	298.15	
Coto et al.[3]	298.15	0.008 - 0.019
Hwang & Robinson[4]	298.15	0.008 - 0.019
Iguchi[5]	298.15	0.015 - 0.019
Kato[6]	298.15	0.015 - 0.019
Lepori & Matteoli[7]	298.15	
Nagai & Ishii[8]	293.15 - 303.15	0.006 - 0.024
Pierotti[9]	299.85 - 300.25	0.009
Scatchard & Satkiewicz[10]	293.15 - 308.15	0.006 - 0.030
Washburn & Handorf[11]	298.15	0.014 - 0.019
Surface tension data		
Myers & Clever[12]	303.15	
cyclohexane + 2-propanol		
VLE data		

Gao et al.[13]	298.15 - 303.15	
Gupta et al.[14]	298.15 - 308.15	0.006 - 0.026
Haase & Tillmann[15]	298.15	0.006 - 0.016
Storonkin & Morachevskii[16]	313.15	0.014 - 0.032
cyclohexane + 1-propanol		
VLE data		
Gupta et al.[14]	298.15 - 308.15	0.003 - 0.022
Hwang & Robinson[4]	298.15	0.003 - 0.014
Iguchi[5]	298.15	0.009 - 0.014
Smirnova & Kurtynina[17]	298.15	0.003 - 0.014
Surface tension data		
Yang & Bae[18]	308.15	
cyclohexane + 1-butanol		
VLE data		
Belabbaci et al.[19]	313.15	0.003 - 0.025
Belabbaci et al.[20]	313.15	0.018
Bhardwaj et al.[21]	298.15	0.002 - 0.021
Huo et al.[22]	303.39 - 308.56	0.015 - 0.022
Smirnova & Kurtynina[17]	298.15 - 308.15	0.002 - 0.021
Surface tension data		
Trieschmann[23]	295.15	
methylcyclohexane + ethanol		
VLE data		
Ishii[24]	293.15 - 303.15	0.007 - 0.016
Kretschmer & Wiebe[25]	308.15	0.016 - 0.02

2 Detailed View of the MD Density Profiles for the Mixture Cyclohexane + Ethanol

As outlined in the main body of this work, the MD density profile results show a peculiar topology, namely a (minor) enrichment of cyclohexane, followed by a (minor) depletion of cyclohexane and a (minor) enrichment of the associating component. These regions are highlighted in in Figure S1. As the position of the enrichment and depletion depends on the liquid mole fraction, the regions are only exemplary highlighted in Figure S1 for one composition.

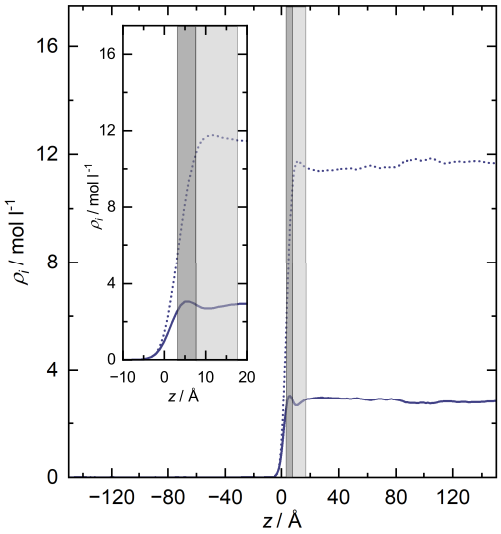

Figure S1: Density profiles of the binary mixture of cyclohexane + ethanol with the liquid mole fraction of cyclohexane $x'_{\mathrm{cyc}} = 0.191$ mol mol^{-1} at $T = 303.15$ K. The dotted lines indicate ethanol and the solid line cyclohexane. The inset shows the interfacial region in more detail. Shown are MD results. The shaded regions highlight the described enrichment/depletion behavior: (Minor) enrichment of cyclohexane (dark gray) followed by a (minor) depletion of cyclohexane and a (minor) enrichment of ethanol (light gray).

3 Influence of Cross-Interaction Influence Parameters β_{ij} on DGT Results

Similar 'type iv' behavior in DGT predictions have been reported by other groups. *Liang et al.*[26] analyzed the mathematical origin of such behavior and identified potential pitfalls associated with the use of the geometric-mean combining rule for the influence parameter. They demonstrated that a numerically robust application of the geometric-mean DGT requires the so-called path function, defined as the sum of the component densities multiplied by the square root of their respective influence parameters, to vary monotonically along the solution profile, which is the case for the studied mixtures within this work. However, sharp density changes, even if the path function appears monotonic, are regarded as a warning sign, since one of the fundamental assumptions of DGT is that density gradients remain small compared to the inverse of the intermolecular distance.[26] *Mairhofer & Gross*[27] investigated the same mixture (hexane + ethanol) using both DFT and DGT and observed a comparable interfacial topology for the DGT results when using geometric mixing rule for the cross-interaction DGT influence parameter, and demonstrated that the steep gradients in the DGT profiles could be largely mitigated by introducing an adjustable cross-influence parameter (β_{ij}), which substantially altered the shape of the underlying density profiles. In the mixtures studied here (cf. Fig. S2 for the mixture of cyclohexane + ethanol), the use of an adjustable parameter β_{ij} – while slightly mitigating steep gradients – did not change the overall topology of the interfacial density profiles. These findings highlight that the occurrence of steep gradients is not unique to the present systems but is a general issue of the underlying approximation of DGT when applied to strongly non-ideal mixtures. The underlying square-gradient approximation may therefore no longer be valid, potentially necessitating higher-order corrections or non-local theories.

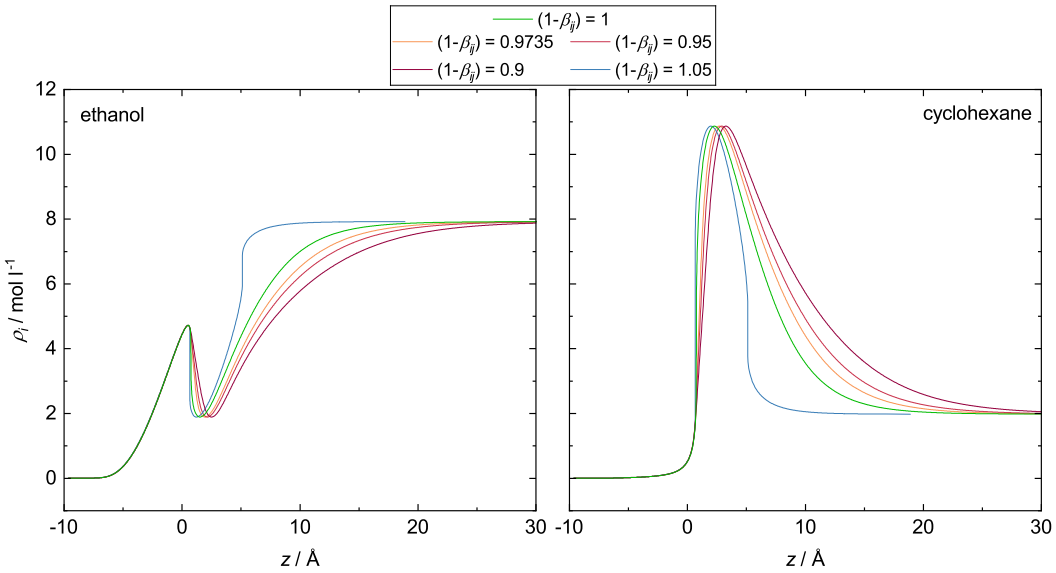

Figure S2: Density profiles of the binary mixture of cyclohexane + ethanol with the liquid mole fraction of cyclohexane $x'_{\text{cyc}} = 0.2$ mol mol^{-1} at $T = 303.15$ K. Results from the PCP-SAFT EOS for the sDGT approach. Color coded are different values of β_{ij}: the geometric mixing rule is shown in green ($(1 - \beta_{ij}) = 1$), adopting the bulk binary interaction parameter ξ_{ij}, i.e. $(1\text{-}\beta_{ij}) = \xi_{ij} = 0.9735$ is shown in orange, $(1\text{-}\beta_{ij}) = 0.95$ and 0.9 are shown in red, and $(1\text{-}\beta_{ij}) = 1.05$ is shown in blue.

4 Comparison of Stabilized DGT and Reference Fluid DGT Algorithm

Fig. S3 compares the density profiles as calculated using the PCP-SAFT EOS in combination with the stabilized DGT (sDGT) algorithm proposed by *Mu et al.*[28] (left) and the reference fluid DGT (RFDGT) approach [29] (right). The results are exemplary shown for the mixture cyclohexane + ethanol with a liquid mole fraction of cyclohexane of $x'_{\text{cyc}} = 0.7$ mol mol^{-1} and a temperature of $T = 303.15$ K. Fig. S3-left shows the iterative convergence using the sDGT approach for the iterations 1 (initialized density profiles), 36, 71, 106, and 141 (being the final converged state). The first iteration shown after the initial guess (green) shows the same qualitative behavior as the final density profile, i.e. there is a significant depletion of cyclohexane at the interface after an initial maximum on the gas side of the interface. The third set of profiles (blue-green) shows only small deviations to the final set of density profiles at around $z = 1$ Å, whereas the fourth iteration is nearly identical to the final density

profiles and is therefore concealed by the final iteration (purple) in Fig. S3-left. The final iteration of the sDGT approach converged to the density profiles of the RFDGT approach (right). Thus the results from the two DGT algorithms are consistent.

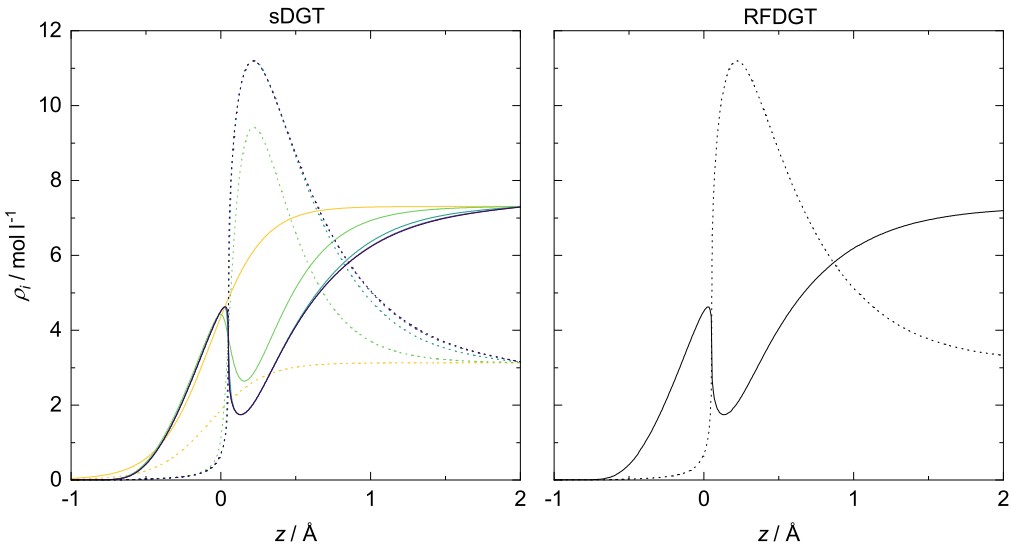

Figure S3: Density profiles of the binary mixture of cyclohexane + ethanol with the liquid mole fraction of cyclohexane $x'_{\mathrm{cyc}} = 0.7$ mol mol^{-1} at $T = 303.15$ K. Results from the PCP-SAFT EOS for the sDGT approach (left) and RFDGT approach (right). The dotted lines indicate ethanol and the solid line cyclohexane. For the sDGT approach, results from 5 iterations are shown color coded (yellow: initial guessed density profiles) to purple (final converged density profiles).

5 Comparison of Experimental VLE Data with EOS Results

Figures S4-S5 compare PCP-SAFT results (with adjusted binary interaction parameters) to experimental VLE data in the specified temperature range. The fitted binary interaction parameters $\xi_{\mathrm{mecyc},j}$ of the methylcyclohexane mixtures are listed in Table S2.

Table S2: PCP-SAFT binary interaction parameter $\xi_{\mathrm{mecyc},j}$ of methylcyclohexane with different alcohol components j.

component j	$\xi_{\mathrm{mecyc},j}$
ethanol	0.9707
2-propanol	0.9771
1-propanol	0.9733
1-butanol	0.9765

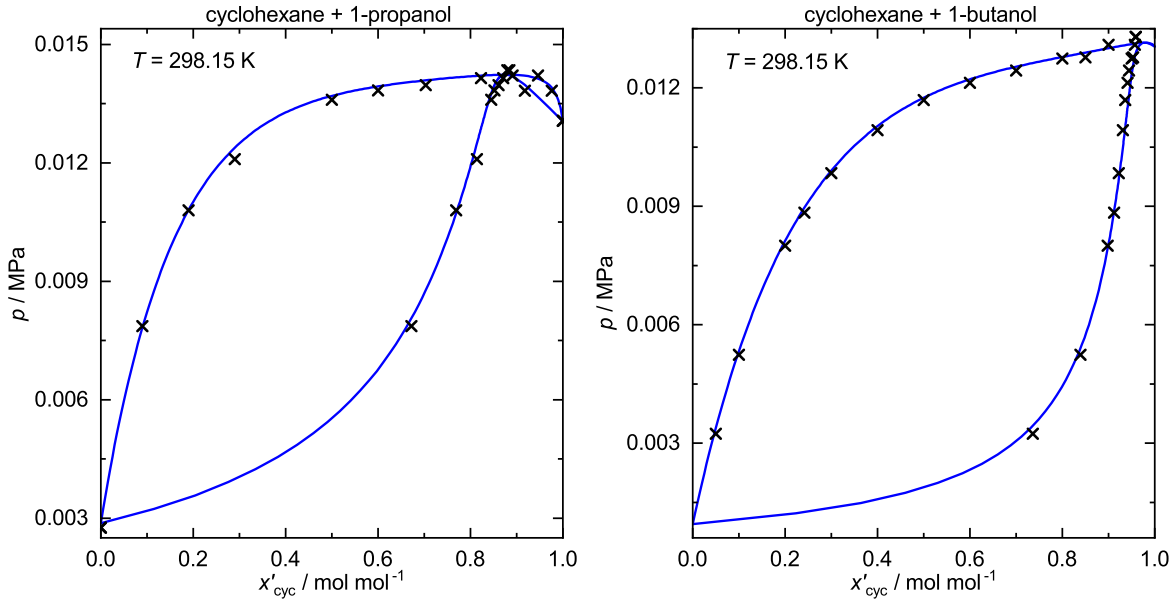

Figure S4: p - x phase diagrams of the binary mixtures cyclohexane + 1-propanol (left) and cyclohexane + 1-butanol (right) at $T = 298.15$ K. The solid blue lines are the results from the PCP-SAFT. The crosses are experimental data from *Smirnova & Kurtynina*.[17]

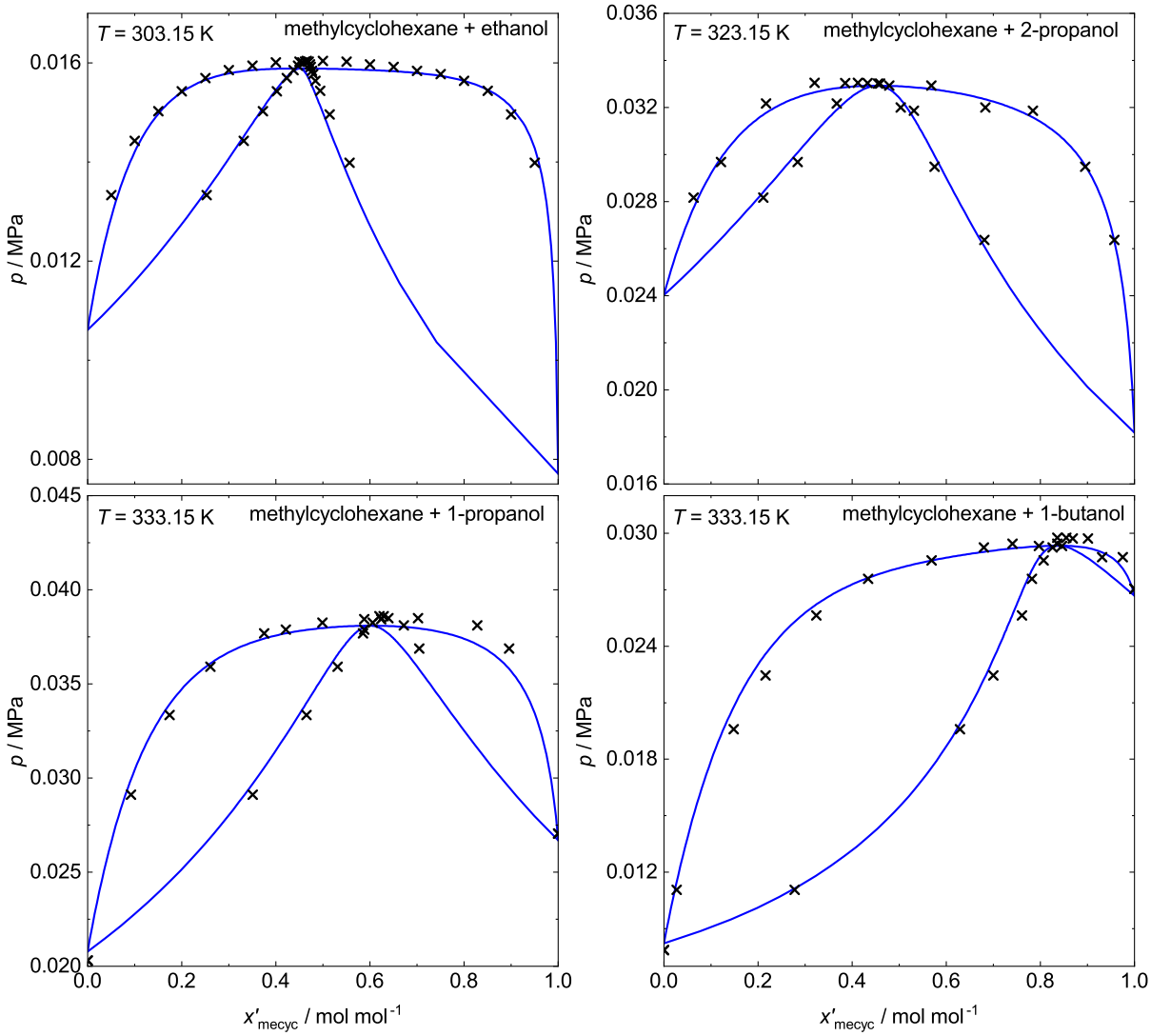

Figure S5: p - x phase diagrams of the binary mixtures methylcyclohexane + ethanol at $T = 303.15$ K (top left), methylcyclohexane + 2-propanol at $T = 323.15$ K (top right), methylcyclohexane + 1-propanol at $T = 333.15$ K (bottom left), and methylcyclohexane + butanol at $T = 333.15$ K (bottom right). The solid blue lines are the results from the PCP-SAFT. The crosses are experimental data from *Ishii*[24] (methylcyclohexane + ethanol), *Nagata el a.*[30] (methylcyclohexane + 2-propanol), *Nagata*[31] (methylcyclohexane + 1-propanol) and *Nagata*[31] (methylcyclohexane + butanol).

6 p-T Projections of the Remaining Mixtures

Figures. S6-S8 present the p-T projections of the phase behavior for the systems cyclohexane + 1-propanol and cyclohexane + 1-butanol, methylcyclohexane + ethanol and methylcyclohexane + 2-propanol, and methylcyclohexane + 1-propanol and methylcyclohexane + 1-butanol, respectively.

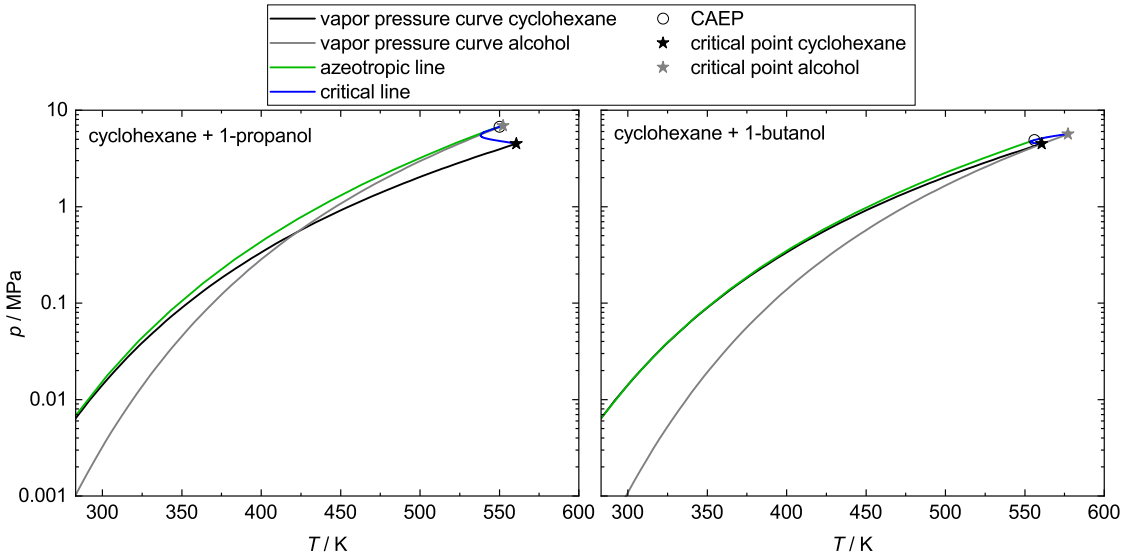

Figure S6: p - T projections of the binary mixtures cyclohexane + 1-propanol (left) and cyclohexane + 1-butanol (right). Shown are results for the PCP-SAFT EOS. Solid black and gray lines are the vapor pressure curves of the pure components; solid green and blue lines are the azeotropic and critical line respectively; the circle represents the critical azeotropic end point (CAEP) and the stars the critical point of the pure components.

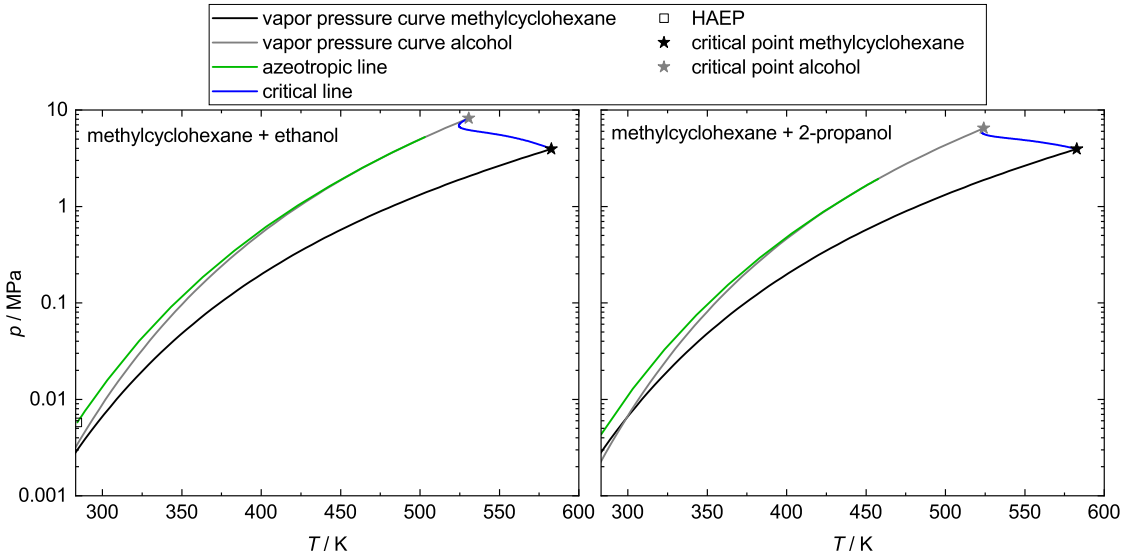

Figure S7: p - T projections of the binary mixtures methylcyclohexane + ethanol (left) and methylcyclohexane + 2-propanol (right). Shown are results for the PCP-SAFT EOS. Solid black and gray lines are the vapor pressure curves of the pure components; solid green and blue lines are the azeotropic and critical line respectively; the square represents the heteroazeotropic end point (HAEP) and the stars the critical point of the pure components.

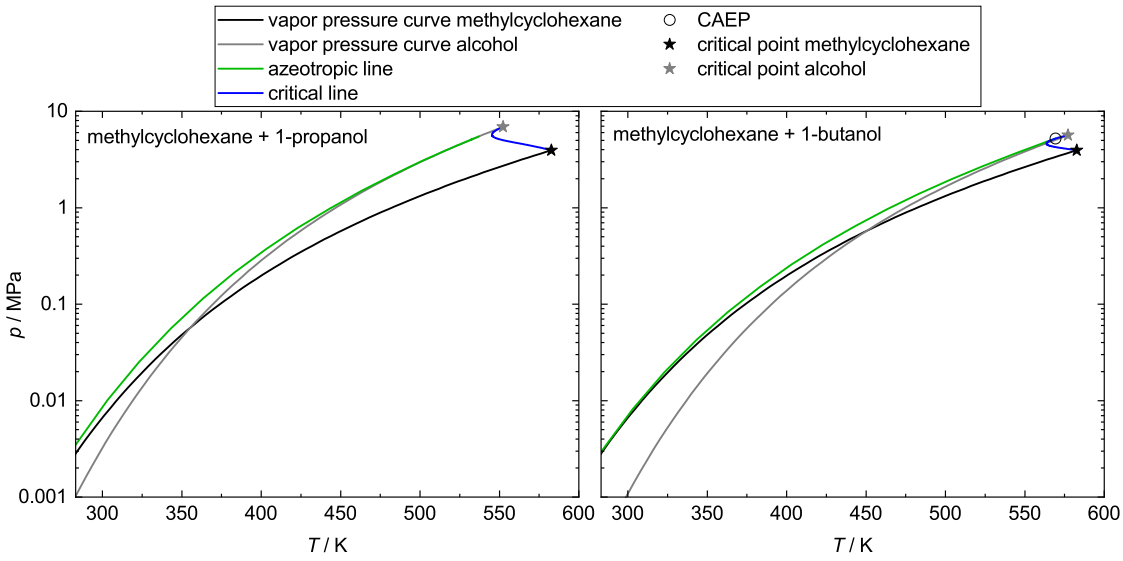

Figure S8: p - T projections of the binary mixtures methylcyclohexane + 1-propanol (left) and methylcyclohexane + 1-butanol (right). Shown are results for the PCP-SAFT EOS. Solid black and gray lines are the vapor pressure curves of the pure components; solid green and blue lines are the azeotropic and critical line respectively; the circle represents the critical azeotropic end point (CAEP) and the stars the critical point of the pure components.

7 Clustering of Alcohol Molecules Studied by MD Simulations

Figure S9 shows snapshots of the MD simulations, exemplary for the mixture of cyclohexane + ethanol at $T = 303.15$ K and $x'_{\mathrm{cyc}} \approx 0.9$ mol mol^{-1}. Fig. S9-A and S9-B show the complete simulation scenario, from the side and front, respectively. Fig. S9-C shows the ethanol molecules alone and Fig. S9-D shows two exemplary chosen ethanol clusters from that simulation snapshot. As can be seen from Figure S9-C, ethanol molecules are enriched near the interface, as was shown in the main body of this work. In particular, it appears that the clusters have a preferential residency in the vicinity of the interface. Figure S9-D shows clusters of associating ethanol molecules in a trimer and pentamer.

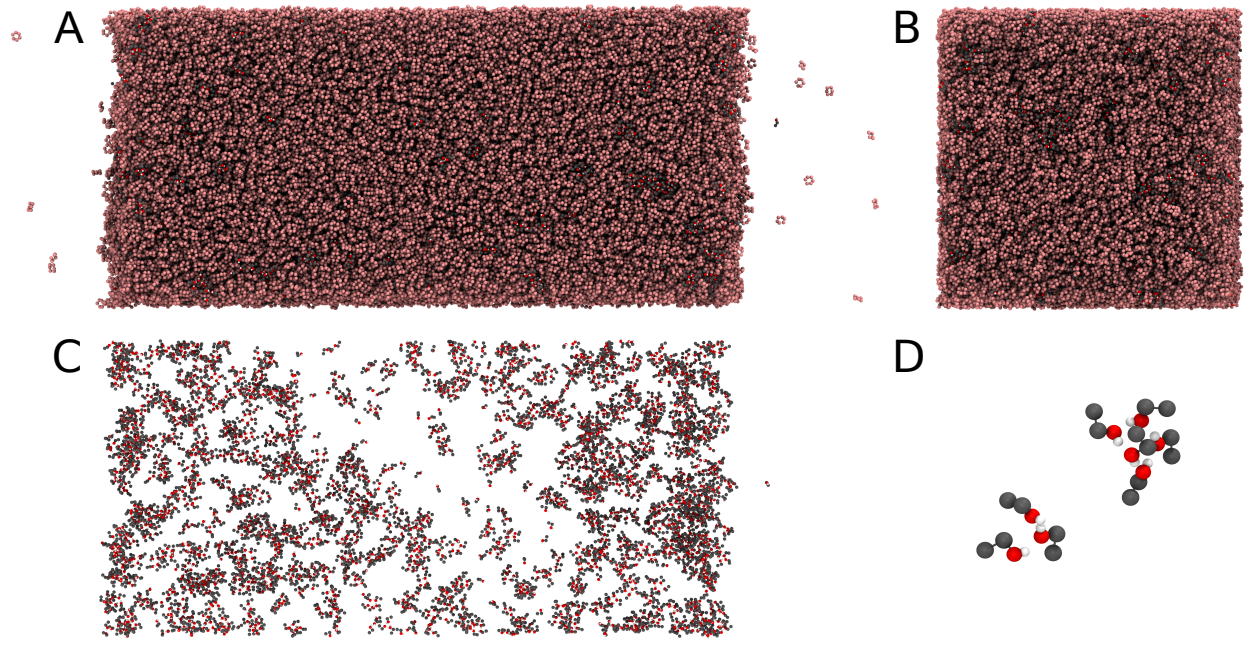

Figure S9: MD simulation snapshots. (A) complete simulation scenario – side view, (B) complete simulation scenario – view on interface, (C) only ethanol molecules – side view, and (D) exemplary chosen clusters. Ethanol C-atoms are shown in gray, O-atoms in red and H-Atoms in white. The six sites of cyclohexane are shown in rose.

8 Detailed Examination of DFT Density Profiles for Cyclohexane + Ethanol

Two subtle elements to the DFT component density profiles were mentioned in the main body of this work, namely: (a) a very small enrichment of the associating component; (b) a minimum in the cyclohexane density profiles after the enrichment peak. This is exemplary shown in Figure S10 for the mixture cyclohexane + ethanol at $T = 303.15$ K and $x'_{\mathrm{cyc}} = 0.038$ mol mol^{-1}. The difference for each component density profile (left: ethanol, right: cyclohexane) to their respective liquid bulk phase density (ρ'_i) is shown.

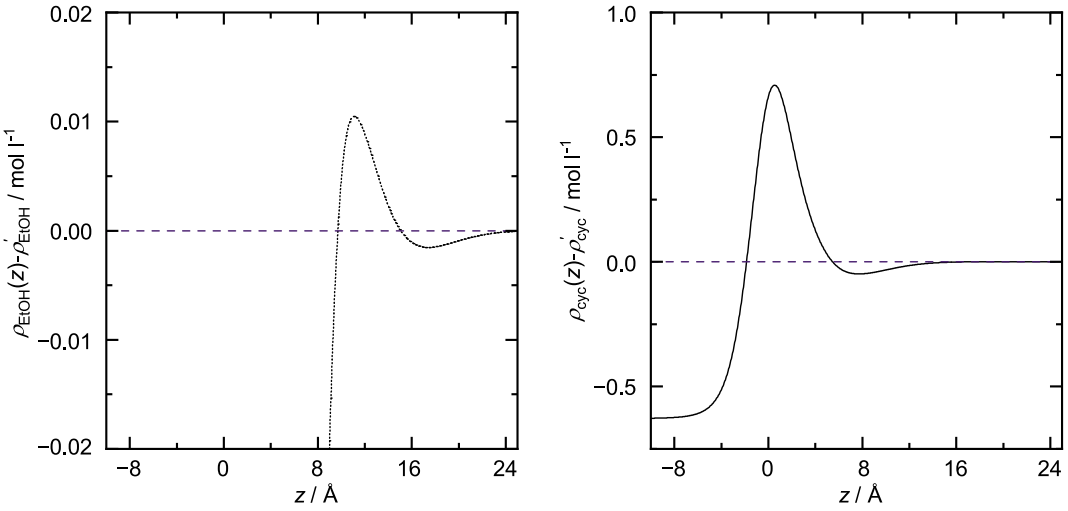

Figure S10: Difference between the DFT component density profiles of ethanol (left) and cyclohexane (right) to their liquid bulk phase density (ρ'_i) for the mixture cyclohexane + ethanol at $T = 303.15$ K and $x'_{\mathrm{cyc}} = 0.038$ mol mol^{-1}.

As outlined in the main body of this work, the DFT results (in contrast to the DGT results) only show a weak maximum in the total density profiles, which is exemplary shown in Figure S11 for the mixture cyclohexane + ethanol at $T = 303.15$ K and $x'_{\mathrm{cyc}} = 0.191$ mol mol^{-1}.

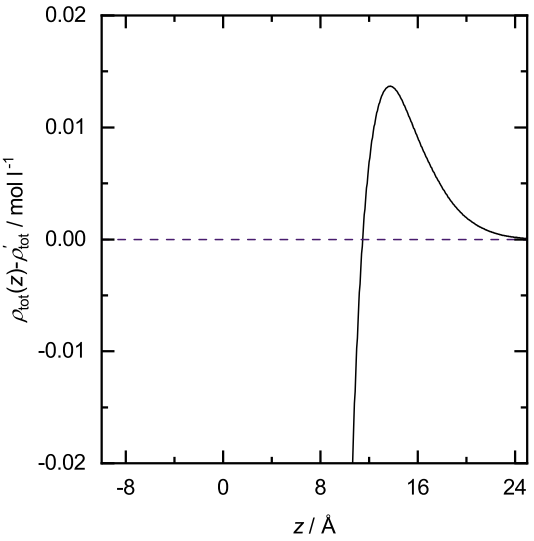

Figure S11: Difference between the DFT total density profiles of the mixture ethanol + cyclohexane to the total liquid bulk phase density (ρ'_{tot}) for the mixture cyclohexane + ethanol at $T = 303.15$ K and $x'_{\mathrm{cyc}} = 0.191$ mol mol^{-1}.

9 Interfacial Properties of the Mixture Cyclohexane + 2-Propanol

A comparison of the interfacial properties calculated from both equations of state in combination with DGT and DFT as well as MD results for the mixture cyclohexane + 2-propanol is presented in Figure S12.

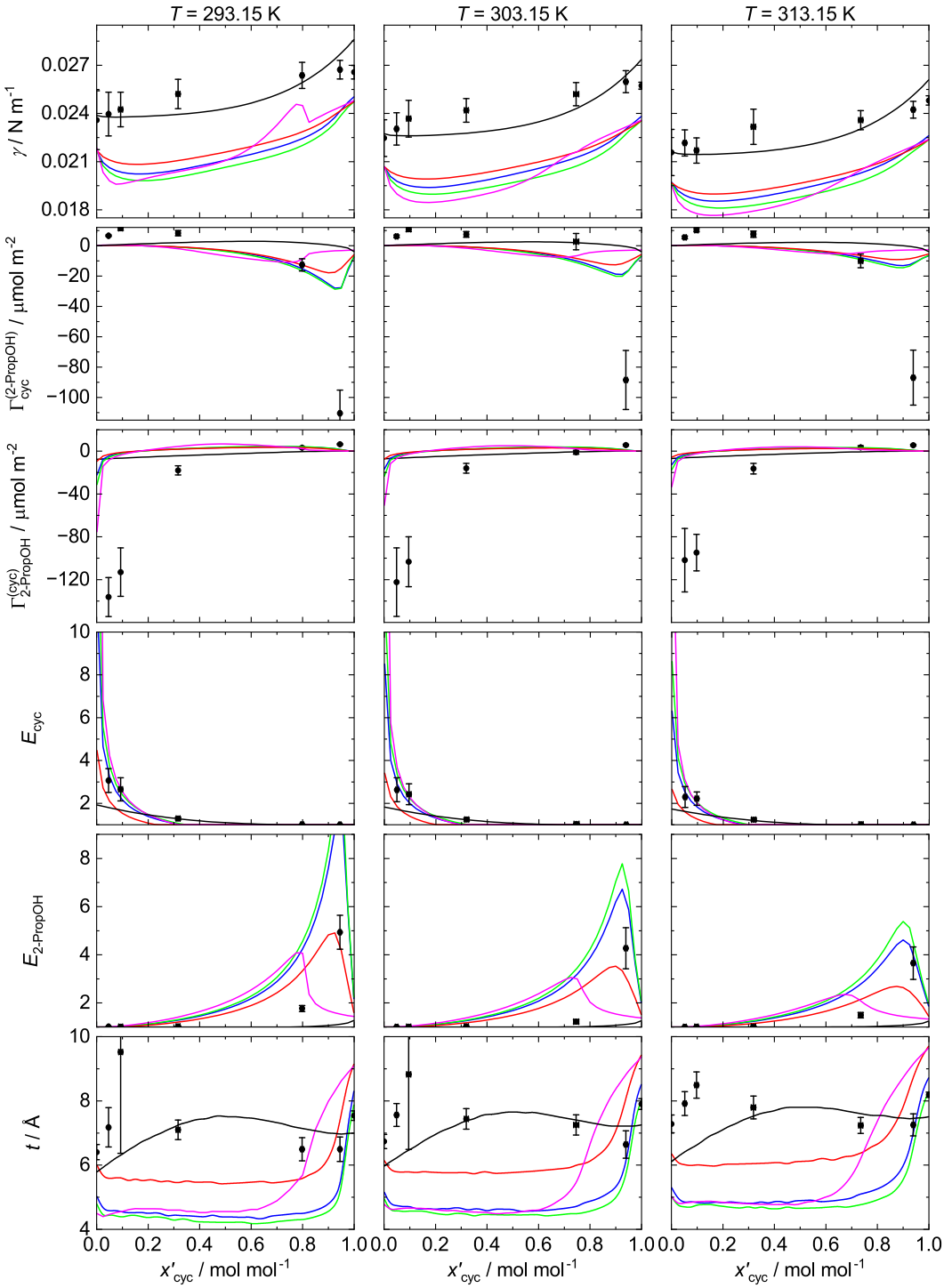

Figure S12: Surface tension (top), relative adsorption (second and third from the top), enrichment (second and third from the bottom) and interfacial thickness (bottom) of the system cyclohexane + 2-propanol as a function of the liquid phase mole fraction of cyclohexane x'_{cyc} at T = 293.15 K, 303.15 K, and 313.15 K, respectively. Black dots are MD results, solid lines are results from PCP-SAFT (blue), SAFT-VR Mie (green), sCPA (red), Peng-Robinson (magenta) EOS + DGT, PCP-SAFT EOS + DFT (black).

10 DGT Component Density Profiles for Cyclohexane + 2-Propanol from Different EOS

The component density profiles of cyclohexane + 2-propanol are compared for the PCP-SAFT, SAFT-VR Mie, sCPA, and Peng-Robinson EOS in Figures S13 and S14. Only DGT results are shown.

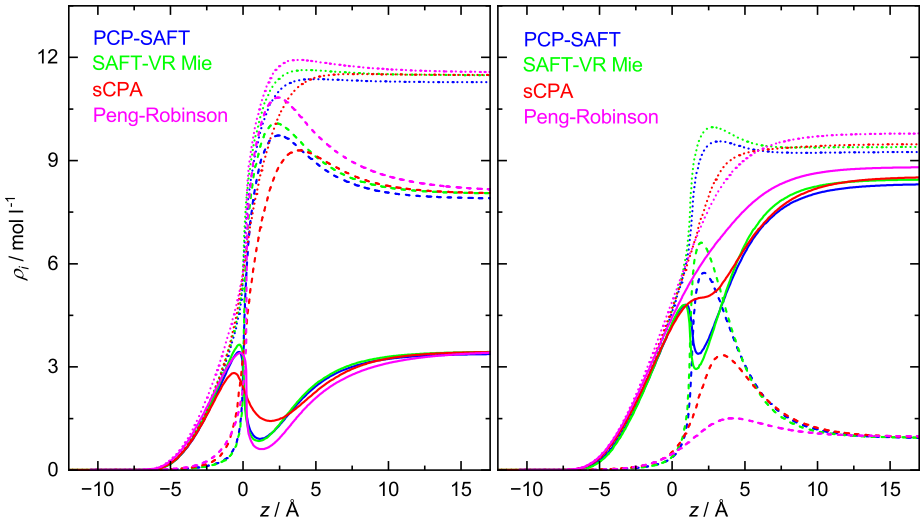

Figure S13: Density profiles of the binary mixture of cyclohexane + 2-propanol at $T = 303.15$ K with different compositions. Results from PCP-SAFT (blue), SAFT-VR Mie (green), sCPA (red), Peng-Robinson (magenta) EOS + DGT. The dashed line indicates 2-propanol, the solid line cyclohexane, and the dotted line the total density. The depicted concentrations are $x'_{\mathrm{cyc}} =$ 0.3 (left), and 0.9 (right) mol mol^{-1}.

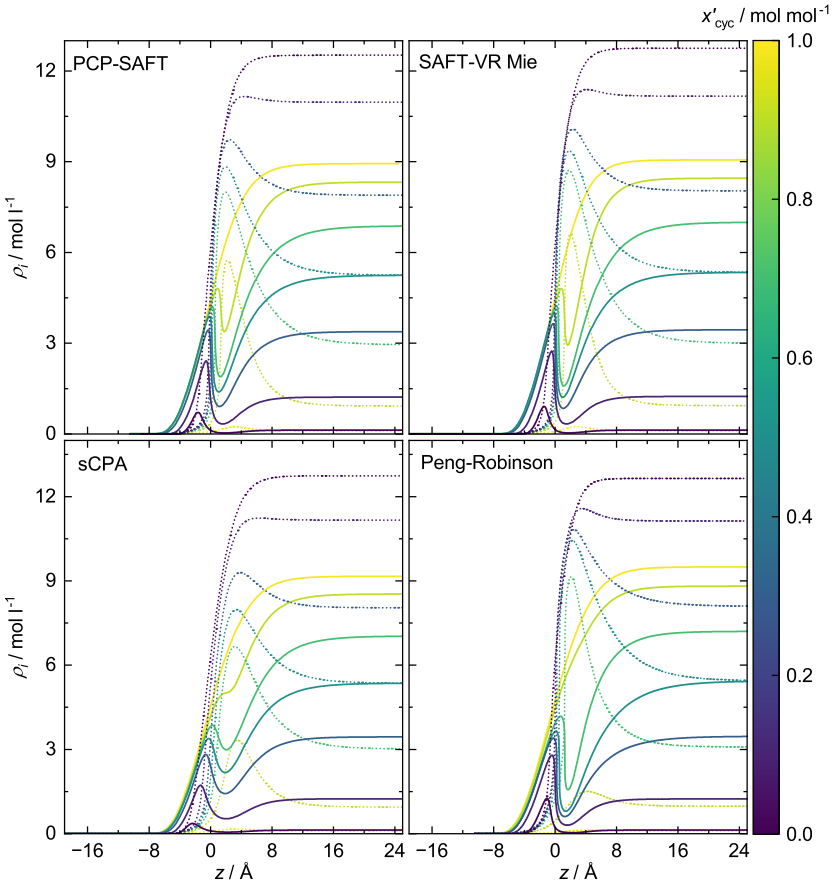

Figure S14: Density profiles of PCP-SAFT EOS (top left), SAFT-VR Mie EOS (top right), sCPA EOS (bottom left), Peng-Robinson EOS (bottom right) + DGT, of the binary mixture of cyclohexane + 2-propanol at $T = 303.15$ K. The liquid phase mole fraction of cyclohexane is color coded. The dotted lines indicate 2-propanol; the solid lines cyclohexane. The depicted concentrations are $x'_{\mathrm{cyc}} = 0.01$, 0.1, 0.3, 0.5, 0.7, 0.9, 0.99 mol mol^{-1}.

11 Component Density Profiles of Additional Mixtures

Figures S15-S26 present the density profiles obtained from DGT and DFT which were mentioned in the main body of this work, but not discussed in detail therein. In Figs. S15-S26, results are shown for the following systems: cyclohexane + 1-propanol; cyclohexane + 1-butanol; methylcyclohexane + ethanol; methylcyclohexane + 2-propanol; methylcyclohexane + 1-propanol; methylcyclohexane + 1-butanol. In each case, results for DGT and DFT at three temperatures are shown. In all cases, the PCP-SAFT EOS was used. The obtained interfacial structures are qualitatively in agreement with the results discussed in the main body of this work.

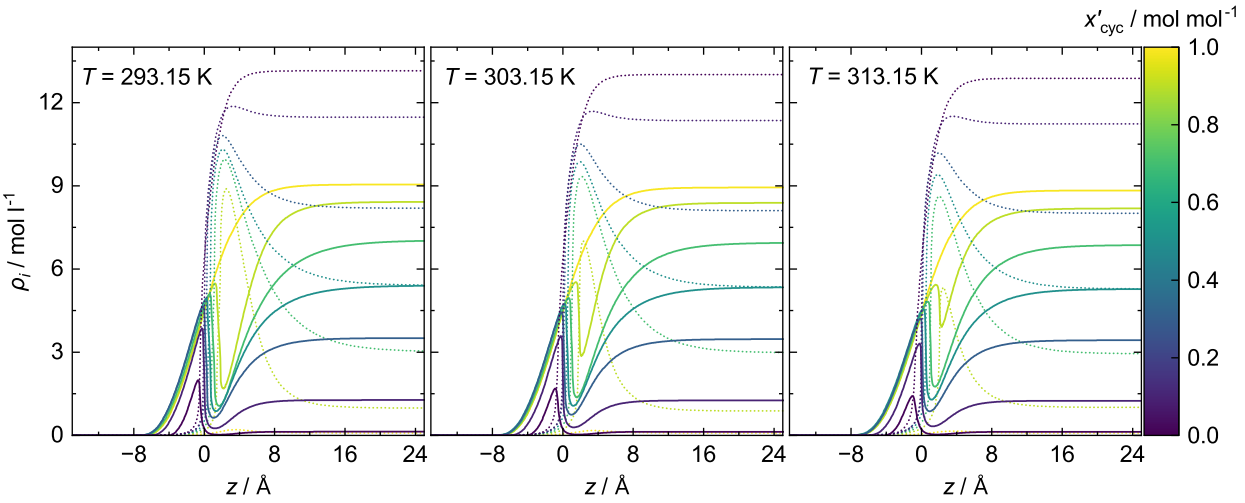

Figure S15: Density profiles of PCP-SAFT EOS + DGT, of the binary mixture of cyclohexane + 1-propanol at $T = 293.15$ K, 303.15 K, and 313.15 K, respectively. The liquid phase mole fraction of cyclohexane is color coded. The dotted lines indicate 1-propanol; the solid lines cyclohexane. The depicted concentrations correspond to a liquid phase mole fraction of cyclohexane of $x'_{\mathrm{cyc}} = 0.01$, 0.1, 0.3, 0.5, 0.7, 0.9, 0.99 mol mol^{-1}.

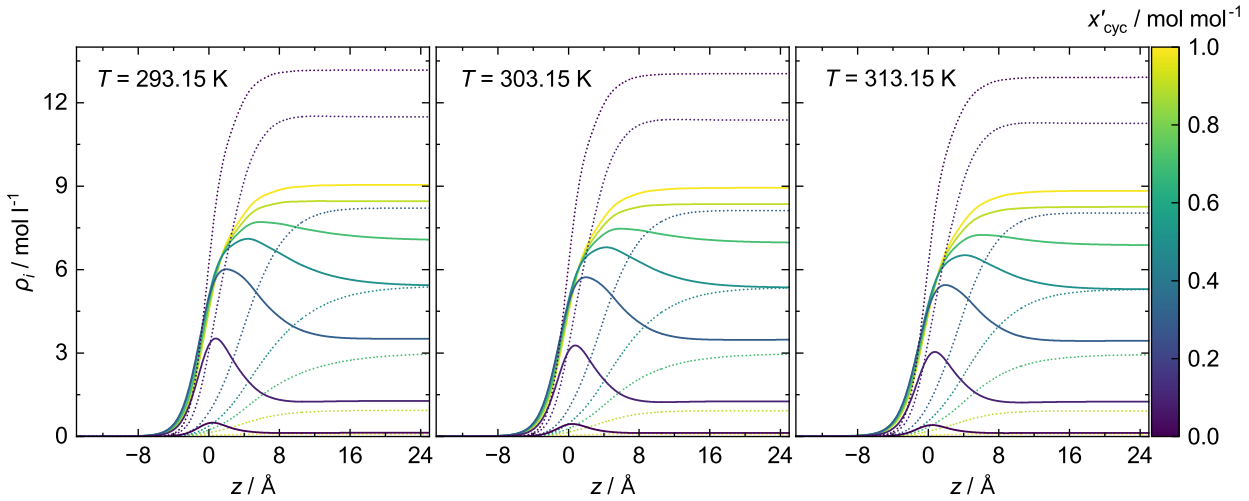

Figure S16: Density profiles of PCP-SAFT EOS + DFT, of the binary mixture of cyclohexane + 1-propanol at $T = 293.15$ K, 303.15 K, and 313.15 K, respectively. The liquid phase mole fraction of cyclohexane is color coded. The dotted lines indicate 1-propanol; the solid lines cyclohexane. The depicted concentrations correspond to a liquid phase mole fraction of cyclohexane of $x'_{cyc} = 0.01$, 0.1, 0.3, 0.5, 0.7, 0.9, 0.99 mol mol^{-1}.

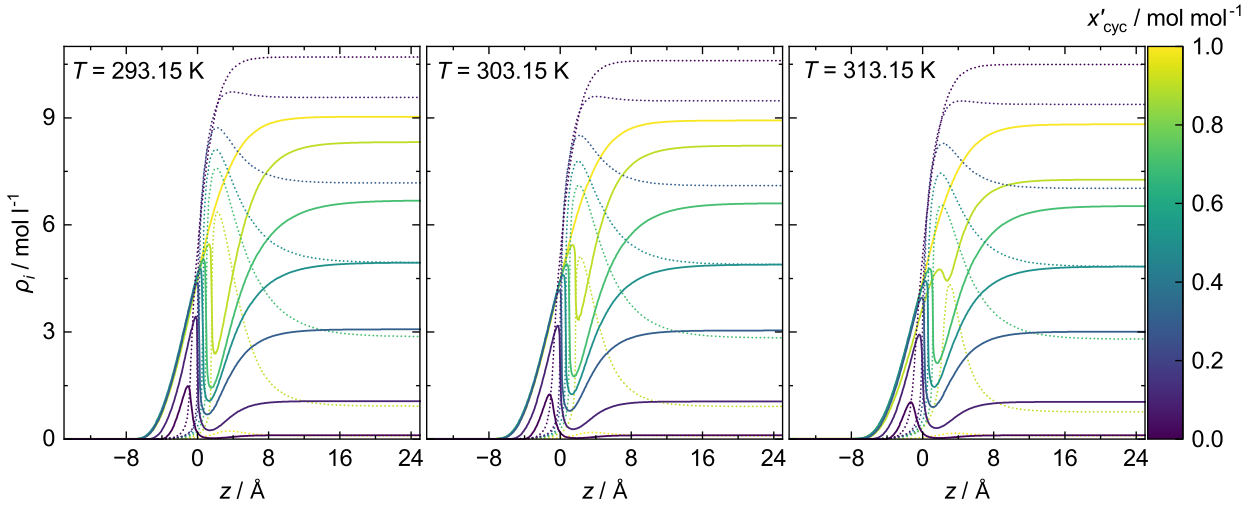

Figure S17: Density profiles of PCP-SAFT EOS + DGT, of the binary mixture of cyclohexane + 1-butanol at $T = 293.15$ K, 303.15 K, and 313.15 K, respectively. The liquid phase mole fraction of cyclohexane is color coded. The dotted lines indicate 1-butanol; the solid lines cyclohexane. The depicted concentrations correspond to a liquid phase mole fraction of cyclohexane of $x'_{cyc} = 0.01$, 0.1, 0.3, 0.5, 0.7, 0.9, 0.99 mol mol^{-1}.

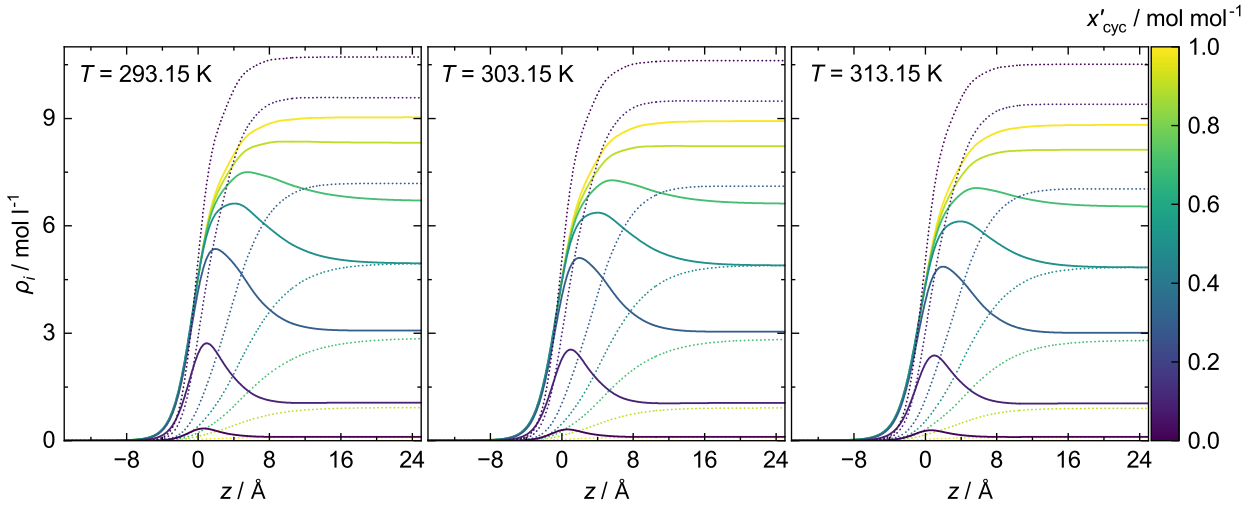

Figure S18: Density profiles of PCP-SAFT EOS + DFT, of the binary mixture of cyclohexane + 1-butanol at $T = 293.15$ K, 303.15 K, and 313.15 K, respectively. The liquid phase mole fraction of cyclohexane is color coded. The dotted lines indicate 1-butanol; the solid lines cyclohexane. The depicted concentrations correspond to a liquid phase mole fraction of cyclohexane of $x'_{\mathrm{cyc}} = 0.01$, 0.1, 0.3, 0.5, 0.7, 0.9, 0.99 mol mol^{-1}.

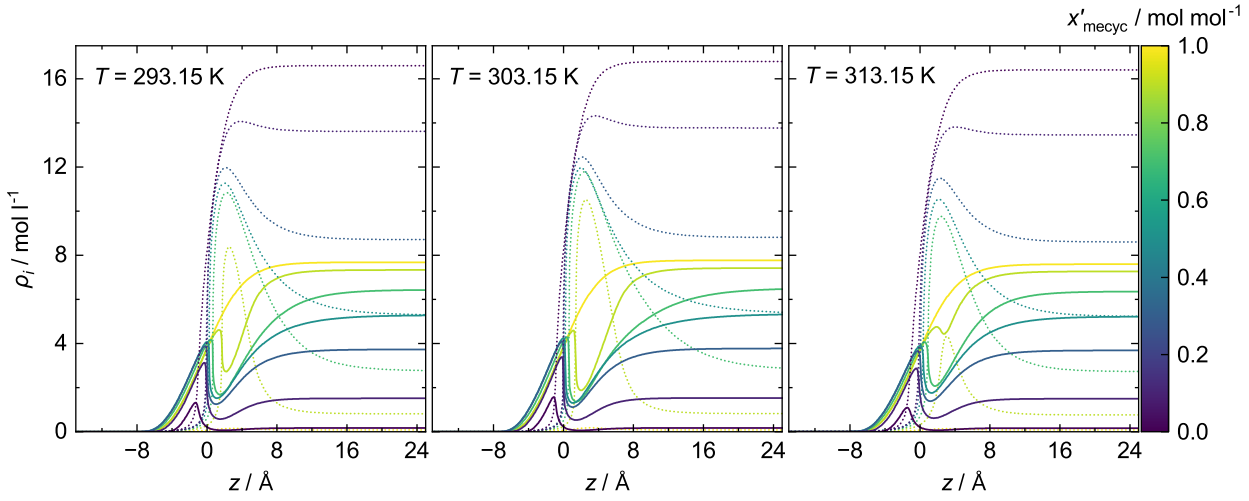

Figure S19: Density profiles of PCP-SAFT EOS + DGT, of the binary mixture of methylcyclohexane + ethanol at $T = 293.15$ K, 303.15 K, and 313.15 K, respectively. The liquid phase mole fraction of methylcyclohexane is color coded. The dotted lines indicate ethanol; the solid lines methylcyclohexane. The depicted concentrations correspond to a liquid phase mole fraction of methylcyclohexane of $x'_{\mathrm{mecyc}} = 0.01$, 0.1, 0.3, 0.5, 0.7, 0.9, 0.99 mol mol^{-1}.

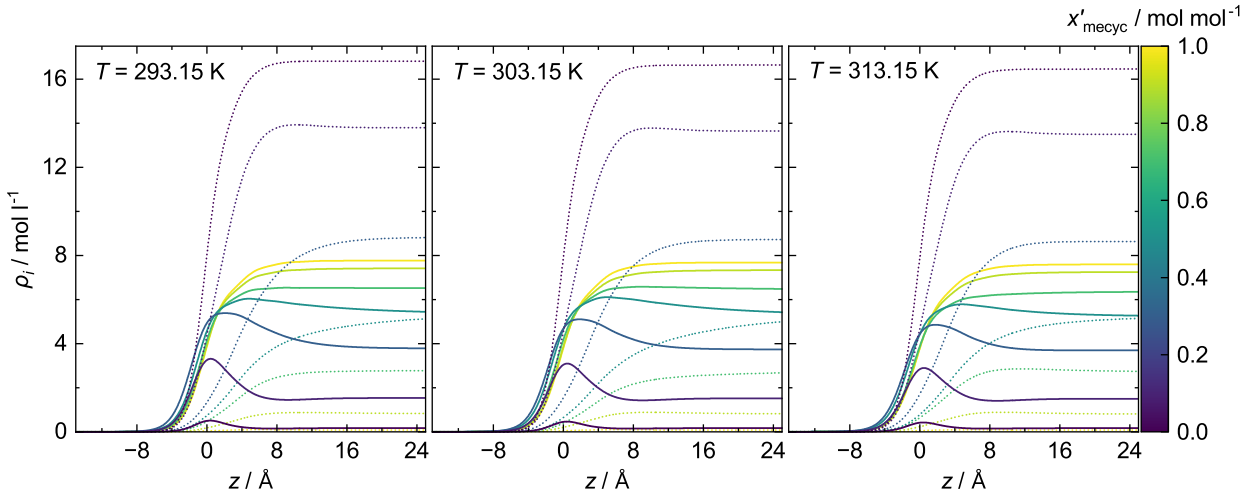

Figure S20: Density profiles of PCP-SAFT EOS + DFT, of the binary mixture of methylcyclohexane + ethanol at $T = 293.15$ K, 303.15 K, and 313.15 K, respectively. The liquid phase mole fraction of methylcyclohexane is color coded. The dotted lines indicate ethanol; the solid lines methylcyclohexane. The depicted concentrations correspond to a liquid phase mole fraction of methylcyclohexane of $x'_{\mathrm{mecyc}} = 0.01$, 0.1, 0.3, 0.5, 0.7, 0.9, 0.99 mol mol^{-1}.

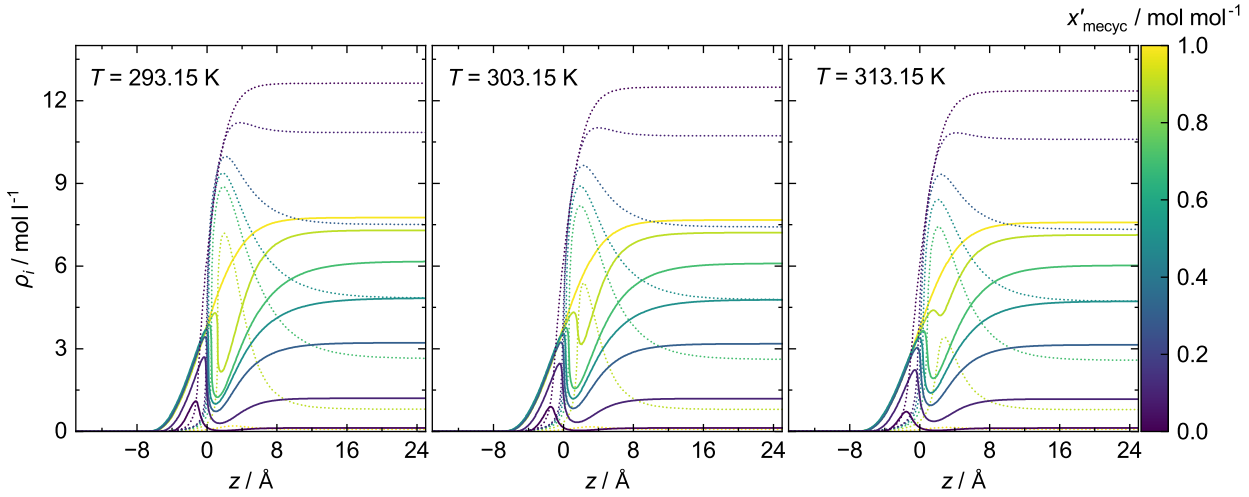

Figure S21: Density profiles of PCP-SAFT EOS + DGT, of the binary mixture of methylcyclohexane + 2-propanol at $T = 293.15$ K, 303.15 K, and 313.15 K, respectively. The liquid phase mole fraction of methylcyclohexane is color coded. The dotted lines indicate 2-propanol; the solid lines methylcyclohexane. The depicted concentrations correspond to a liquid phase mole fraction of methylcyclohexane of $x'_{\mathrm{mecyc}} = 0.01$, 0.1, 0.3, 0.5, 0.7, 0.9, 0.99 mol mol^{-1}.

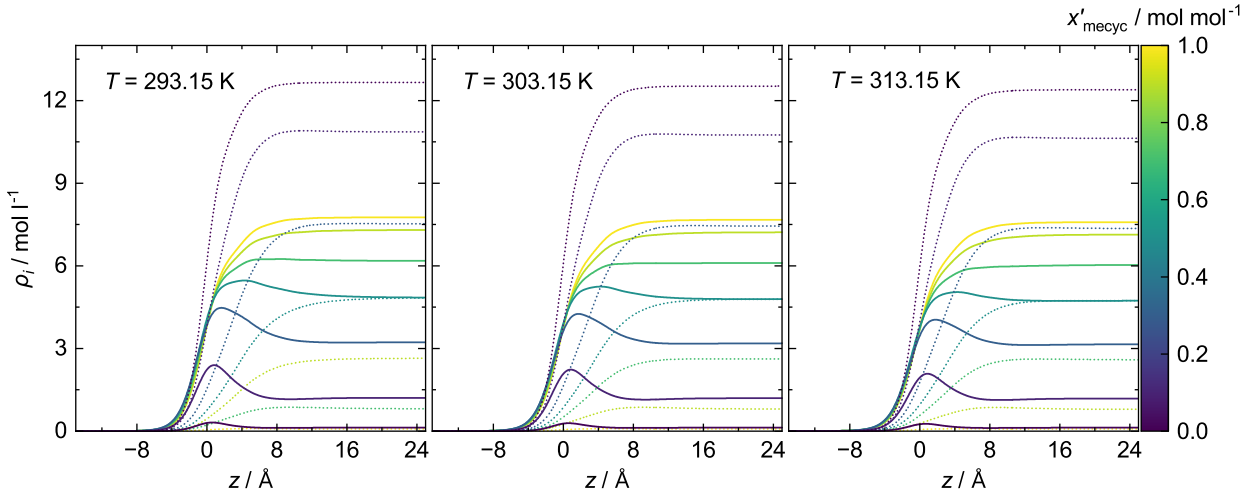

Figure S22: Density profiles of PCP-SAFT EOS + DFT, of the binary mixture of methylcyclohexane + 2-propanol at $T = 293.15$ K, 303.15 K, and 313.15 K, respectively. The liquid phase mole fraction of methylcyclohexane is color coded. The dotted lines indicate 2-propanol; the solid lines methylcyclohexane. The depicted concentrations correspond to a liquid phase mole fraction of methylcyclohexane of $x'_{\mathrm{mecyc}} = 0.01$, 0.1, 0.3, 0.5, 0.7, 0.9, 0.99 mol mol^{-1}.

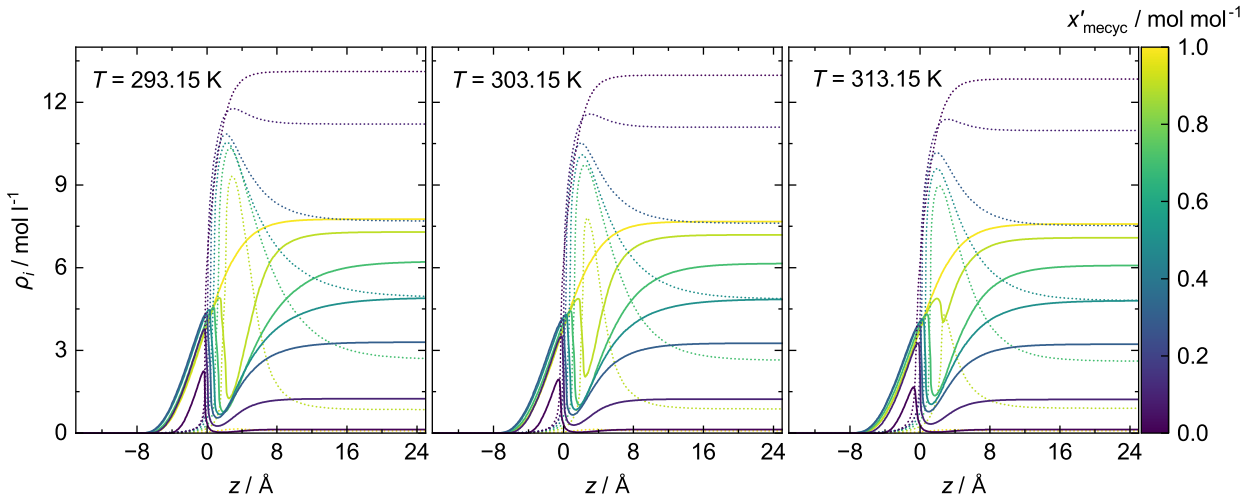

Figure S23: Density profiles of PCP-SAFT EOS + DGT, of the binary mixture of methylcyclohexane + 1-propanol at $T = 293.15$ K, 303.15 K, and 313.15 K, respectively. The liquid phase mole fraction of methylcyclohexane is color coded. The dotted lines indicate 1-propanol; the solid lines methylcyclohexane. The depicted concentrations correspond to a liquid phase mole fraction of methylcyclohexane of $x'_{\mathrm{mecyc}} = 0.01$, 0.1, 0.3, 0.5, 0.7, 0.9, 0.99 mol mol^{-1}.

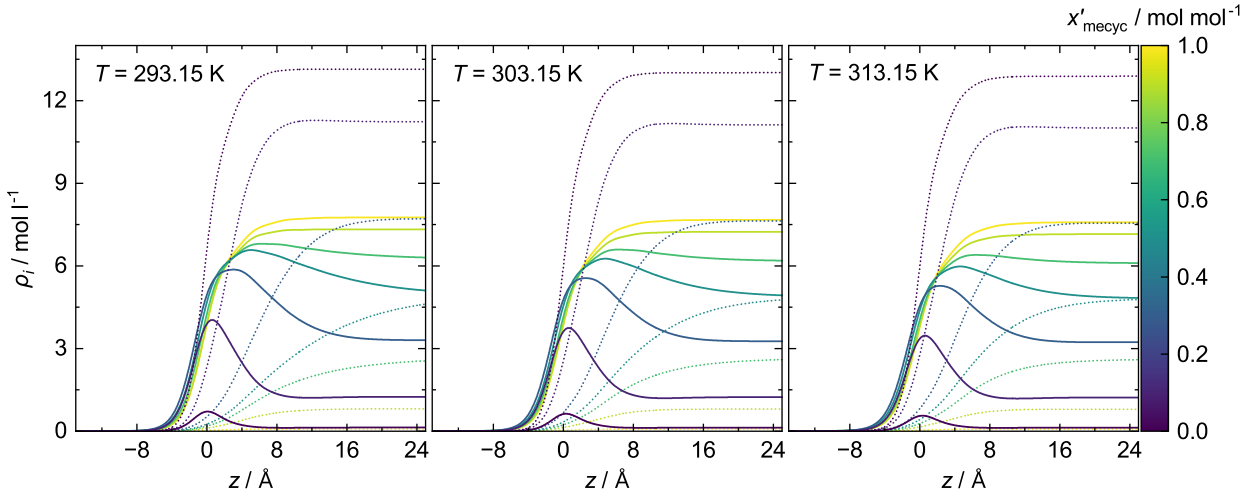

Figure S24: Density profiles of PCP-SAFT EOS + DFT, of the binary mixture of methylcyclohexane + 1-propanol at $T = 293.15$ K, 303.15 K, and 313.15 K, respectively. The liquid phase mole fraction of methylcyclohexane is color coded. The dotted lines indicate 1-propanol; the solid lines methylcyclohexane. The depicted concentrations correspond to a liquid phase mole fraction of methylcyclohexane of $x'_{\mathrm{mecyc}} = 0.01$, 0.1, 0.3, 0.5, 0.7, 0.9, 0.99 mol mol^{-1}.

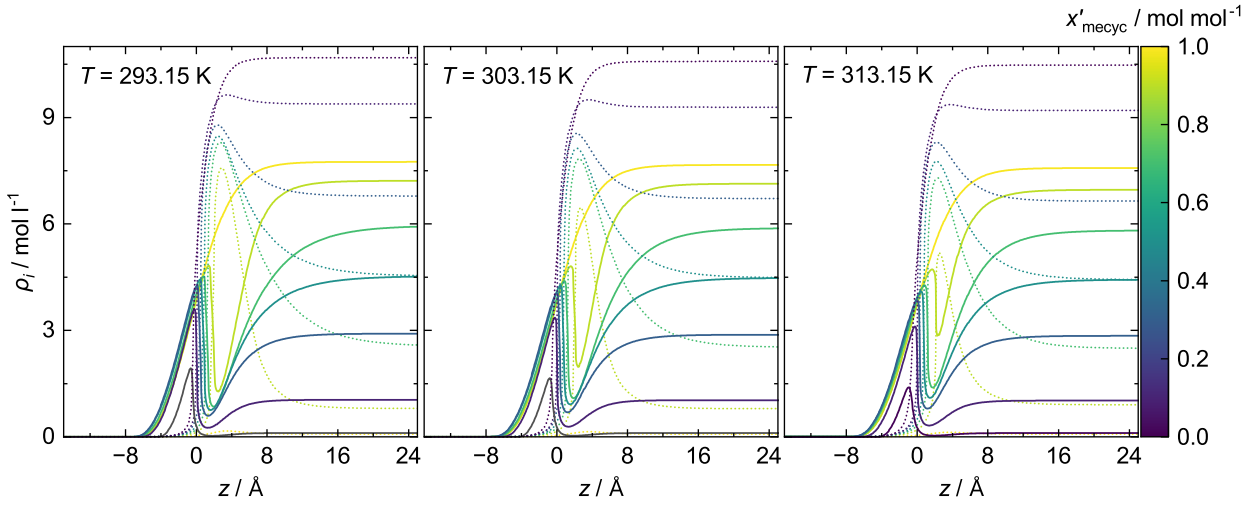

Figure S25: Density profiles of PCP-SAFT EOS + DGT, of the binary mixture of methylcyclohexane + 1-butanol at $T = 293.15$ K, 303.15 K, and 313.15 K, respectively. The liquid phase mole fraction of methylcyclohexane is color coded. The dotted lines indicate 1-butanol; the solid lines methylcyclohexane. The depicted concentrations correspond to a liquid phase mole fraction of methylcyclohexane of $x'_{\mathrm{mecyc}} = 0.01$, 0.1, 0.3, 0.5, 0.7, 0.9, 0.99 mol mol^{-1}.

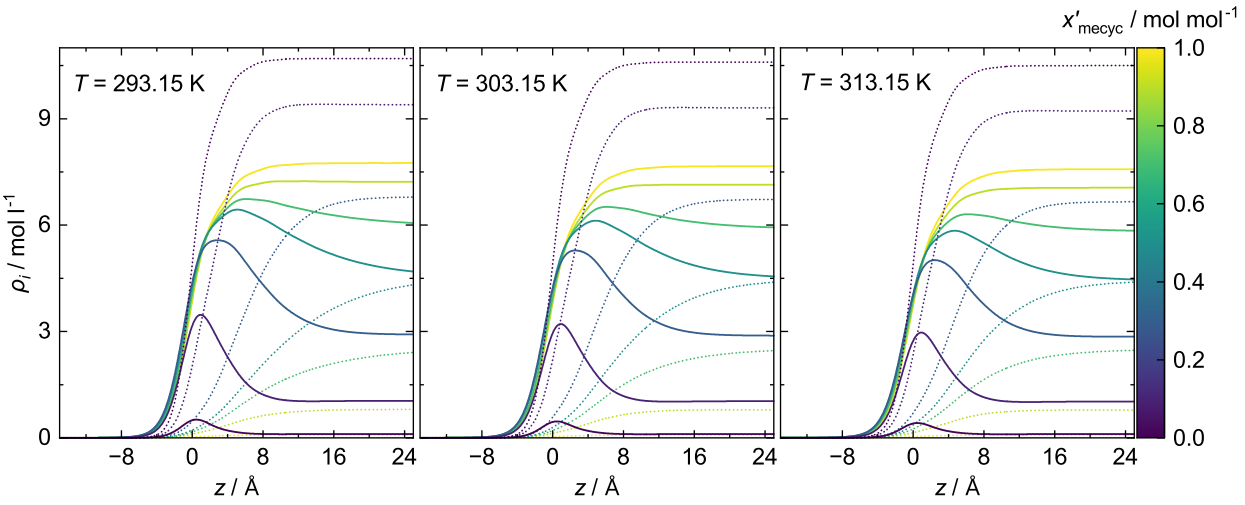

Figure S26: Density profiles of PCP-SAFT EOS + DFT, of the binary mixture of methylcyclohexane + 1-butanol at $T = 293.15$ K, 303.15 K, and 313.15 K, respectively. The liquid phase mole fraction of methylcyclohexane is color coded. The dotted lines indicate 1-butanol; the solid lines methylcyclohexane. The depicted concentrations correspond to a liquid phase mole fraction of methylcyclohexane of $x'_{\mathrm{mecyc}} = 0.01$, 0.1, 0.3, 0.5, 0.7, 0.9, 0.99 mol mol^{-1}.

12 Described Kinks in the Component Density Profiles for the sCPA and Peng-Robinson EOS as the Type 'iv' Behavior Changes to a Monotonic Transition

As outlined in the main body of this work, a kink in the interfacial properties is obtained for the mixture cyclohexane + ethanol for the sCPA and Peng-Robinson EOS, as the 'type iv' behavior changes to a monotonic transition. This kink is also observed for the Peng-Robinson EOS and the mixture cyclohexane + 2-propanol (cf. Fig. S12). Fig. S27 shows this transition exemplary for the mixture cyclohexane + ethanol and for the temperature of 293.15 K. For the sCPA (left) this change occurs near pure cyclohexane, whereas for the Peng-Robinson (right) it occurs at approximately $x'_{\mathrm{cyc}} = 0.7$ mol mol^{-1}.

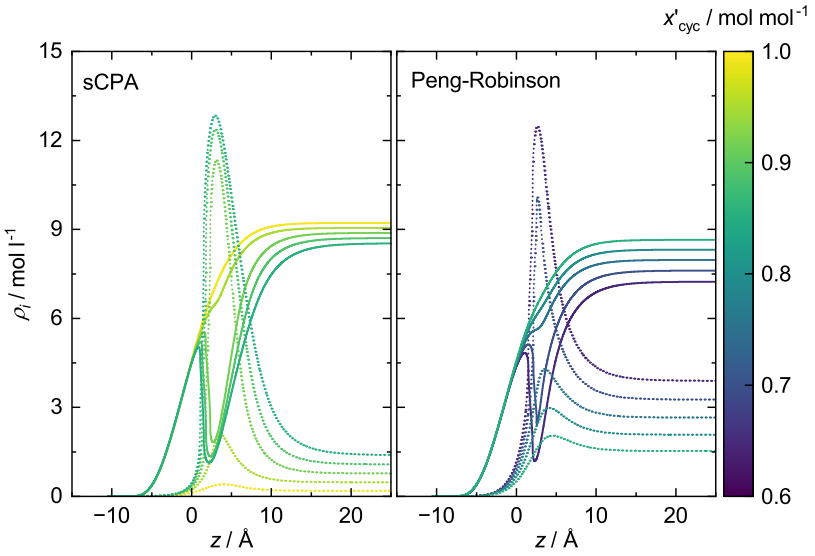

Figure S27: Density profiles of the binary mixture of cyclohexane + ethanol at $T = 293.15$ K. Color coded is the liquid mole fraction of cyclohexane x'_{cyc} in the range of 0.6 to 1 mol mol^{-1}. The dotted lines indicate ethanol; the solid lines cyclohexane. Shown are DGT results for the sCPA EOS (left) and Peng-Robinson EOS (right).

13 Numerical Values of the MD Results for the Mixtures Cyclohexane + Ethanol and Cyclohexane + 2-Propanol

The numerical results of the MD simulations shown in the main body of this work for the mixture cyclohexane + ethanol and cyclohexane + 2-propanol are given in the following tables. Tables S3-S4 list the numerical results for the mixture cyclohexane + ethanol. The results for the mixture cyclohexane + 2-propanol are listed in Tables S5-S6. For both mixtures the tables are structured such that the bulk phase properties are shown in one table and the interfacial properties corresponding to these simulations are shown in a second table.

Table S3: MD results for the vapor-liquid bulk phase properties of the mixture cyclohexane + ethanol. The columns are from left to right: Temperature, pressure, liquid phase concentration, vapor phase concentration, liquid bulk phase density, vapor bulk phase density. The number in the parentheses indicates the statistical uncertainty in the last decimal digits.

T / K	p / MPa	x'_{cyc} / mol mol^{-1}	x''_{cyc} / mol mol^{-1}	ρ' / mol l^{-1}	ρ'' / mol l^{-1}
293.15	0.0138(16)	0	0	9.21(0)	0.0058(7)
	0.0140(23)	0.052(4)	0.246(45)	9.44(2)	0.0058(10)
	0.0143(23)	0.388(6)	0.316(60)	11.20(4)	0.0059(10)
	0.0148(17)	0.584(4)	0.312(61)	12.59(3)	0.0061(7)
	0.0126(24)	0.812(5)	0.371(77)	14.76(6)	0.0052(10)
	0.0112(17)	0.924(3)	0.430(98)	16.15(4)	0.0047(7)
	0.0096(21)	0.962(2)	0.537(89)	16.69(2)	0.0040(9)
	0.0057(13)	1	1	17.25(0)	0.0023(5)
303.15	0.0205(9)	0	0	9.10(0)	0.0083(4)
	0.0229(28)	0.052(4)	0.292(45)	9.31(2)	0.0093(12)
	0.0217(33)	0.391(7)	0.335(55)	11.08(4)	0.0087(13)
	0.0228(32)	0.588(5)	0.336(39)	12.47(4)	0.0092(13)
	0.0207(22)	0.809(2)	0.392(60)	14.55(3)	0.0083(9)
	0.0182(20)	0.922(3)	0.466(69)	15.93(4)	0.0073(8)
	0.0156(23)	0.962(2)	0.592(75)	16.48(3)	0.0062(9)
	0.0111(17)	1	1	17.05(1)	0.0045(6)
313.15	0.0259(25)	0	0	8.99(0)	0.0101(9)
	0.0345(43)	0.054(7)	0.331(34)	9.22(3)	0.0136(18)
	0.0359(52)	0.396(9)	0.352(43)	10.97(6)	0.0142(22)
	0.0337(31)	0.593(4)	0.386(31)	12.35(3)	0.0132(12)
	0.0322(24)	0.808(3)	0.443(42)	14.36(4)	0.0126(10)
	0.0293(32)	0.922(4)	0.522(55)	15.74(5)	0.0115(13)
	0.0247(29)	0.961(2)	0.641(74)	16.27(3)	0.0097(12)
	0.0158(19)	1	1	16.84(0)	0.0062(7)

Table S4: MD results for the vapor-liquid interfacial properties of the mixture cyclohexane + ethanol. The columns are from left to right: Temperature, pressure, liquid phase concentration, surface tension, relative adsorption of both components, enrichment of both components, and interfacial thickness. The number in the parentheses indicates the statistical uncertainty in the last decimal digits.

T / K	p / MPa	x'_{cyc} / mol mol^{-1}	γ / mN m^{-1}	$\Gamma_{\mathrm{cyc}}^{(\mathrm{2-PropOH})}$ / μmol m^{-2}	$\Gamma_{\mathrm{2-PropOH}}^{(\mathrm{cyc})}$ / μmol m^{-2}	E_{cyc}	$E_{\mathrm{2-PropOH}}$	t / Å
293.15	0.0138(16)	0	26.6(4)	–	–	–	–	7.54(15)
	0.0140(23)	0.052(4)	27.3(7)	−128.0(19.0)	7.0(5)	1.01(0)	4.50(80)	6.47(37)
	0.0143(23)	0.388(6)	27.1(6)	−5.2(2.7)	3.2(1.6)	1.02(1)	1.18(7)	6.94(37)
	0.0148(17)	0.584(4)	27.2(8)	−4.9(1.4)	6.9(1.9)	1.03(1)	1.11(3)	6.95(32)
	0.0126(24)	0.812(5)	27.4(1.2)	3.1(1.4)	−13.5(6.5)	1.15(5)	1.03(1)	7.41(38)
	0.0112(17)	0.924(3)	27.8(1.5)	5.9(7)	−72.2(11.0)	1.79(22)	1.01(0)	7.73(56)
	0.0096(21)	0.962(2)	27.8(1.6)	3.1(4)	−79.7(13.5)	2.00(23)	1.01(0)	6.99(35)
	0.0057(13)	1	28.7(1.6)	–	–	–	–	6.19(26)
303.15	0.0205(9)	0	25.7(2)	–	–	–	–	7.90(17)
	0.0229(28)	0.052(4)	25.9(6)	−130.9(20.5)	7.1(6)	1.01(0)	4.45(79)	6.64(27)
	0.0217(33)	0.391(7)	26.1(9)	−3.5(2.7)	2.2(1.7)	1.03(1)	1.16(4)	7.34(37)
	0.0228(32)	0.588(5)	26.2(8)	−3.6(1.7)	5.0(2.4)	1.03(1)	1.12(3)	7.41(40)
	0.0207(22)	0.809(2)	26.5(9)	2.2(6)	−9.5(2.5)	1.13(4)	1.03(1)	7.60(39)
	0.0182(20)	0.922(3)	26.6(1.1)	5.5(6)	−65.7(9.6)	1.70(16)	1.01(0)	7.90(39)
	0.0156(23)	0.962(2)	26.9(1.2)	3.0(5)	−76.1(16.3)	1.88(23)	1.01(0)	7.26(25)
	0.0111(17)	1	26.8(6)	–	–	–	–	6.54(21)
313.15	0.0259(25)	0	24.8(3)	–	–	–	–	8.19(8)
	0.0345(43)	0.054(7)	24.6(7)	−123.0(30.8)	6.8(9)	1.01(0)	4.09(1.03)	7.12(32)
	0.0359(52)	0.396(9)	24.5(5)	−1.7(3.9)	1.0(2.5)	1.03(2)	1.14(6)	7.84(41)
	0.0337(31)	0.593(4)	24.6(8)	−2.0(1.1)	2.9(1.6)	1.03(1)	1.08(2)	7.70(32)
	0.0322(24)	0.808(3)	24.8(1.0)	2.1(9)	−8.9(4.1)	1.10(3)	1.02(1)	7.77(36)
	0.0293(32)	0.922(4)	25.2(1.0)	5.5(1.0)	−65.8(15.7)	1.64(22)	1.01(0)	8.23(53)
	0.0247(29)	0.961(2)	25.7(1.1)	2.8(6)	−71.6(18.7)	1.75(27)	1.01(0)	7.34(33)
	0.0158(19)	1	25.4(1.1)	–	–	–	–	6.71(19)

Table S5: MD results for the vapor-liquid bulk phase properties of the mixture cyclohexane + 2-propanol. The columns are from left to right: Temperature, pressure, liquid phase concentration, vapor phase concentration, liquid bulk phase density, vapor bulk phase density. The number in the parentheses indicates the statistical uncertainty in the last decimal digits.

T / K	p / MPa	x'_{cyc} / mol mol^{-1}	x''_{cyc} / mol mol^{-1}	ρ' / mol l^{-1}	ρ'' / mol l^{-1}
	0.0138(16)	0	0	9.21(0)	0.0058(7)
	0.0117(18)	0.055(4)	0.188(49)	9.44(9)	0.0049(8)
	0.0122(17)	0.202(5)	0.209(54)	9.75(4)	0.0051(7)
293.15	0.0116(20)	0.684(8)	0.271(81)	11.48(2)	0.0048(9)
	0.0109(18)	0.907(7)	0.329(67)	12.55(4)	0.0045(7)
	0.0088(17)	0.954(3)	0.415(79)	12.80(2)	0.0036(7)
	0.0042(12)	1	1	13.06(0)	0.0018(5)
	0.0205(9)	0	0	9.10(0)	0.0083(4)
	0.0173(50)	0.061(5)	0.199(43)	9.26(4)	0.0070(20)
	0.0207(24)	0.254(10)	0.206(43)	9.81(3)	0.0084(10)
303.15	0.0198(33)	0.681(8)	0.304(48)	11.33(3)	0.0080(14)
	0.0171(22)	0.904(8)	0.364(67)	12.39(4)	0.0069(9)
	0.0145(24)	0.951(5)	0.448(71)	12.64(3)	0.0058(10)
	0.0079(17)	1	1	12.92(0)	0.0032(7)
	0.0259(25)	0	0	8.99(0)	0.0101(9)
	0.0309(28)	0.061(5)	0.223(34)	9.16(3)	0.0122(12)
	0.0318(37)	0.265(8)	0.272(45)	9.70(3)	0.0125(15)
313.15	0.0307(41)	0.682(9)	0.340(52)	11.13(7)	0.0122(20)
	0.0317(31)	0.903(7)	0.397(78)	12.23(3)	0.0125(12)
	0.0229(27)	0.948(5)	0.563(56)	12.47(3)	0.0091(12)
	0.0133(27)	1	1	12.76(0)	0.0052(11)

Table S6: MD results for the vapor-liquid interfacial properties of the mixture cyclohexane + 2-propanol. The columns are from left to right: Temperature, pressure, liquid phase concentration, surface tension, relative adsorption of both components, enrichment of both components, and interfacial thickness. The number in the parentheses indicates the statistical uncertainty in the last decimal digits.

T / K	p / MPa	x'_{cyc} / mol mol^{-1}	γ / mN m^{-1}	$\Gamma_{\mathrm{cyc}}^{(\mathrm{2-PropOH})}$ / μmol m^{-2}	$\Gamma_{\mathrm{2-PropOH}}^{(\mathrm{cyc})}$ / μmol m^{-2}	E_{cyc}	$E_{\mathrm{2-PropOH}}$	t / Å
	0.0138(16)	0	26.6(4)	–	–	–	–	7.54(15)
	0.0117(18)	0.055(4)	26.7(6)	−110.5(15.3)	6.5(5)	1.00(0)	4.94(70)	6.49(38)
	0.0122(17)	0.202(5)	26.4(8)	−12.7(4.0)	3.2(9)	1.02(1)	1.77(12)	6.49(36)
293.15	0.0116(20)	0.684(8)	25.2(9)	8.2(1.7)	−17.9(4.3)	1.29(7)	1.03(1)	7.10(31)
	0.0109(18)	0.907(7)	24.2(1.1)	11.4(1.4)	−113.0(22.6)	2.66(54)	1.01(0)	9.52(3.15)
	0.0088(17)	0.954(3)	24.0(1.4)	6.6(5)	−136.3(18.2)	3.06(56)	1.01(0)	7.18(61)
	0.0042(12)	1	23.6(1.8)	–	–	–	–	6.41(24)
	0.0205(9)	0	25.7(2)	–	–	–	–	7.90(17)
	0.0173(50)	0.061(5)	26.7(6)	−88.5(19.5)	5.6(7)	1.01(0)	4.27(85)	6.64(43)
	0.0207(24)	0.254(10)	26.4(8)	2.7(5.4)	−1.0(1.8)	1.04(2)	1.22(9)	7.25(32)
303.15	0.0198(33)	0.681(8)	25.2(9)	7.4(1.9)	−16.0(4.6)	1.24(7)	1.02(1)	7.44(32)
	0.0171(22)	0.904(8)	24.2(1.1)	10.8(1.5)	−103.3(23.4)	2.43(49)	1.01(0)	8.83(2.33)
	0.0145(24)	0.951(5)	24.0(1.4)	6.1(1.0)	−122.4(32.0)	2.63(56)	1.01(0)	7.56(36)
	0.0079(17)	1	22.5(1.1)	–	–	–	–	6.74(22)
	0.0259(25)	0	24.8(3)	–	–	–	–	8.19(8)
	0.0309(28)	0.061(5)	26.7(6)	−87.0(18.1)	5.6(7)	1.01(0)	3.66(67)	7.25(34)
	0.0318(37)	0.265(8)	26.4(8)	−10.0(4.5)	3.6(1.5)	1.02(1)	1.49(11)	7.23(25)
313.15	0.0307(41)	0.682(9)	25.2(9)	7.5(2.1)	−16.3(5.0)	1.24(7)	1.02(1)	7.79(36)
	0.0317(31)	0.903(7)	24.2(1.1)	10.2(1.2)	−94.7(17.1)	2.22(31)	1.01(0)	8.49(41)
	0.0229(27)	0.948(5)	24.0(1.4)	5.4(1.0)	−101.8(29.7)	2.30(49)	1.01(0)	7.92(37)
	0.0133(27)	1	21.6(1.4)	–	–	–	–	7.28(28)

14 Numerical Values of All Component Density Profiles at the Molecular Simulation Composition

The numerical values of all component density profiles (at the molecular simulation composition) shown in the main body of this work are given in the electronic Supplementary Information. They are structured as .csv tables labeled with the method (MS, DFT, or DGT), the investigated mixture, and corresponding temperature. The values for the z-coordinate are shifted, such that $z(\rho_{50}^{\mathrm{tot}}) = 0$ at $\rho_{50}^{\mathrm{tot}} = \rho_{\mathrm{tot}}'' + 0.5(\rho_{\mathrm{tot}}' - \rho_{\mathrm{tot}}'')$ (see main body of this work).

References

(1) Matteoli, E.; Lepori, L. Excess Gibbs free energies of (tetrachloromethane + an alcohol or a cyclic ether) at 298.15 K. *J. Chem. Thermodyn.* **1986**, *18*, 1065–1076.

(2) Cancellu, D.; Marongiu, B.; Porcedda, S. Excess gibbs free energies of mixtures of substances containing nitrogen groups. *Thermochim. Acta* **1991**, *178*, 33–49.

(3) Coto, B.; Pando, C.; Rubio, R. G.; Renuncio, J. A. R. Vapour-liquid equilibrium of the ethanol–propanal system. *J. Chem. Soc., Faraday Trans.* **1995**, *91*, 273–278.

(4) Hwang, S.-c.; Robinson, R. L. J. Vapor-liquid equilibriums at 25.ETA. for nine alcohol-hydrocarbon binary systems. *J. Chem. Eng. Data* **1977**, *22*, 319–325.

(5) Iguchi, A. Vapor-liquid equilibrium at 25 C for binary systems between alcohols and hydrocarbons. *Kagaku Sochi* **1978**, *20*, 66–68.

(6) Kato, M. Analysis of the Excess Gibbs Energies of Binary Mixtures Using Non-Randomness Factors Determined from Excess Volume Data. *Bull. Chem. Soc. Jpn.* **1982**, *55*, 23–27.

(7) Lepori, L.; Matteoli, E. Excess Gibbs energies of the ternary system ehtanol + tetrahydrofuran + cyclohexane at 298.15 K. *Fluid Phase Equilib.* **1997**, *134*, 113–131.

(8) Nagai, Y.; Isii, N. Studies on Volatility of Fuels Containing Ethyl Alcohol (II) Calculation of Starting Temperatures of an Engine when using Ethyl Alcohol-Ethyl Ether Mixtures as its Fuel. *Proc. Imp. Acad.* **1934**, *10*, 650–653.

(9) Pierotti, G. J.; Deal, C. H.; Derr, E. L. Activity Coefficients and Molecular Structure. *Ind. Eng. Chem.* **1959**, *51*, 95–102.

(10) Scatchard, G.; Satkiewicz, F. G. Vapor-Liquid Equilibrium. XII. The System Ethanol-Cyclohexane from 5 to 65°. *J. Am. Chem. Soc.* **1964**, *86*, 130–133.

(11) Washburn, E. R.; Handorf, B. H. The Vapor Pressure of Binary Solutions of Ethyl Alcohol and Cyclohexane at 25°. *J. Am. Chem. Soc.* **1935**, *57*, 441–443.

(12) Myers, R. S.; Clever, H. L. The Surface Tension and Density of some Hydrocarbon + Alcohol Mixtures at 303.15 K. *J. Chem. Thermodyn.* **1974**, *6*, 949–955.

(13) Gao, P.; Zhang, J.; Peng, Q.; Zhang, J.; Glezakou, V.-A. General Protocol for the Accurate Prediction of Molecular 13C/1H NMR Chemical Shifts via Machine Learning Augmented DFT. *J. Chem. Inf. Model.* **2020**, *60*, 3746–3754.

(14) Gupta, V.; Maken, S.; Kalra, K. C.; Singh, K. C. Molar excess free energy of mixing of 1-propanol or 2-propanol with cyclohexane at 298.15 and 308.15 K in terms of association model with a Flory contribution term. *Fluid Phase Equilib.* **1996**, *120*, 195–203.

(15) Haase, R.; Tillmann, W. Mixing Properties of the Liquid System 2-Propanol + Cyclohexane. *Z. Phys. Chem.* **1995**, *189*, 81–88.

(16) Storonkin, A. V.; Morachevskii, A. G. On the Vapor-Liquid Equilibrium in the System Benzene - Cyclohexane - Isopropyl Alcohol. *Zh. Fiz. Khim.* **1956**, *30*, 1297–1307.

(17) Smirnova, N. A.; Kurtynina, L. M. Thermodynamic Functions of Mixing for a Number of Binary Alcohol - Hydrocarbon Solutions. *Zh. Fiz. Khim.* **1969**, *43*, 1883–1885.

(18) Yang, H. E.; Bae, Y. C. Thermodynamic analysis of phase equilibrium and surface tension of ternary polymer solutions. *AIChE J.* **2019**, *65*, e16679.

(19) Belabbaci, A.; Villamañan, R. M.; Negadi, L.; Martin, C. M.; Ait Kaci, A.; Villamañan, M. a. Vapor–Liquid Equilibria of Binary Mixtures Containing 1-Butanol and Hydrocarbons at 313.15 K. *J. Chem. Eng. Data* **2012**, *57*, 114–119.

(20) Belabbaci, A.; Ghezouali, C.; Villamañán, R. M.; Moreau, A.; Negadi, L.; Villamañán, M. A. P-x isothermal equilibrium data for two ternary systems containing long-chain bioalcohols: (1-butanol or 2-butanol + cyclohexane + methylbenzene) at 313.15 K. *J. Chem. Thermodyn.* **2020**, *141*, 105984.

(21) Bhardwaj, U.; Singh, K.; Maken, S. Molar Excess Free Energy of Mixing of an Isomer of Butanol with Cyclohexane at 308.15 K in Terms of an Association Model with a Flory Contribution Term. *Indian J. Chem. - Section A* **1997**, *36*, 693–696.

(22) Huo, Y.; Xia, S.; Yi, S.; Ma, P. Measurement and correlation of vapor pressure of benzene and thiophene with [BMIM][PF6] and [BMIM][BF4] ionic liquids. *Fluid Phase Equilib.* **2009**, *276*, 46–52.

(23) Trieschmann, H.-G. Oberflächenspannung und Solvatation. *Z. Phys. Chem.* **1935**, *29*, 328–334.

(24) Ishii, N. Studies on Volatility of Fuels Containing Ethyl Alcohol V-VI. *J. Soc. Chem. Ind., Jpn.* **1935**, *38*, 659–25271068.

(25) Kretschmer, C. B.; Wiebe, R. Liquid–Vapor Equilibrium of Ethanol–Methylcyclohexane Solutions. *J. Am. Chem. Soc.* **1949**, *71*, 3176–3179.

(26) Liang, X.; Michelsen, M. L.; Kontogeorgis, G. M. Pitfalls of Using the Geometric-Mean Combining Rule in the Density Gradient Theory. *Fluid Phase Equilib.* **2016**, *415*, 75–83.

(27) Mairhofer, J.; Gross, J. Modeling Properties of the One-Dimensional Vapor-Liquid Interface: Application of Classical Density Functional and Density Gradient Theory. *Fluid Phase Equilib.* **2018**, *458*, 243–252.

(28) Mu, X.; Frank, F.; Alpak, F. O.; Chapman, W. G. Stabilized Density Gradient Theory Algorithm for Modeling Interfacial Properties of Pure and Mixed Systems. *Fluid Phase Equilib.* **2017**, *435*, 118–130.

(29) Miqueu, C.; Mendiboure, B.; Graciaa, A.; Lachaise, J. Modeling of the Surface Tension of Multicomponent Mixtures with the Gradient Theory of Fluid Interfaces. *Ind. Eng. Chem. Res.* **2005**, *44*, 3321–3329.

(30) Nagata, I.; Ohta, T.; Uchiyama, Y. Excess Gibbs free energies for binary systems. Isopropyl alcohol with benzene, cyclohexane, methylcyclohexane. *J. Chem. Eng. Data* **1973**, *18*, 54–59.

(31) Nagata, I. Isothermal vapour-liquid equilibria for binary mixtures of methylcyclohexane with alcohols. *Thermochim. Acta* **1989**, *144*, 95–107.